

Published in final edited form as:

*Oncogene*. 2013 February 21; 32(8): . doi:10.1038/onc.2012.109.

## Disrupting the PIKE-A/Akt interaction inhibits glioblastoma cell survival, migration, invasion and colony formation

Q Qi<sup>1</sup>, K He<sup>1</sup>, X Liu<sup>1</sup>, C Pham<sup>2</sup>, C Meyerkord<sup>2,3</sup>, H Fu<sup>2,3</sup>, and K Ye<sup>1</sup>

<sup>1</sup>Department of Pathology and Laboratory Medicine, Emory University, Atlanta, GA, USA

<sup>2</sup>Department of Pharmacology, Emory University, Atlanta, GA, USA

<sup>3</sup>Emory Chemical Biology Discovery Center, Emory University, Atlanta, GA, USA

### Abstract

The cyclin-dependent kinase 4 (CDK4) amplicon is frequently amplified in numerous human cancers including gliomas. PIKE-A, a proto-oncogene that is one of the important components of the CDK4 amplicon, binds to and enhances the kinase activity of Akt, thereby promoting cancer progression. To define the roles of the PIKE-A/Akt interaction in glioblastoma multiform (GBM) progression, we used biochemical protein/protein interaction (PPI) assays and live cell fluorescence-based protein complementation assays to search for small peptide antagonist from these proteins that were able to block their interaction. Here, we show that disruption of the interaction between PIKE-A and Akt by the small peptides significantly reduces glioblastoma cell proliferation, colony formation, migration and invasion. Disruption of PIKE-A/Akt association potently suppressed GBM cell proliferation and sensitized the cells to two clinical drugs that are currently used to treat GBM. Interestingly, GBM cells containing the CDK4 amplicon were more responsive to the inhibition of the PIKE-A/Akt interaction than GBM cells lacking this amplicon. Taken together, our findings provide proof-of-principle that blocking a PPI that is essential for cancer progression provides a valuable strategy for therapeutic discovery.

### Keywords

glioblastoma; protein/protein interaction; PIKE-A; Akt

### INTRODUCTION

Glioblastoma multiform (GBM), the most common type of primary brain tumors, are highly aggressive, infiltrative and destructive. Recently, radiotherapy plus concomitant and adjuvant temozolomide (TMZ) was shown to significantly improve the survival of GBM patients without reducing their quality of life.<sup>1,2</sup> However, the aggressive nature of glioblastomas renders current treatments, the median survival after treatment is 14 months. Therefore, novel and effective therapeutic interventions for GBM are urgently needed. For this reason, tremendous effort has been spent to identify tumorigenic or tumor-promoting

© 2012 Macmillan Publishers Limited All rights reserved

Correspondence: Dr K Ye, Department of Pathology and Laboratory Medicine, Emory University, 615 Michael street, Atlanta, GA 30300, USA. kye@emory.edu.

#### CONFLICT OF INTEREST

The authors declare no conflict of interest.

Supplementary Information accompanies the paper on the *Oncogene* website (<http://www.nature.com/onc>)

genomic events and molecular pathways that directly drive malignant transformation and tumor progression.

GBM comprehensive genomic profiles mapped by The Cancer Genome Atlas project reveal that one of the most common copy-number alterations in GBM is amplification at chromosome 12q13.3-14.1. This amplification is also observed in many other human cancers including melanoma, breast cancers and lung cancers.<sup>3-7</sup> Importantly, glioblastoma patients harboring this amplification had markedly decreased survival. The cyclin-dependent kinase 4 (*CDK4*) gene has been postulated as the target of this amplification. *CDK4* promotes proliferation by inhibiting the Rb1 tumor suppressor and by sequestering p27Kip1 and p21Cip1, thereby promoting E2F- and Cdk2-dependent cell cycle progression.<sup>8</sup> However, *CDK4* overexpression alone does not induce spontaneous tumorigenesis in transgenic animal models, suggesting that *CDK4* cooperates with other genetic changes to initiate tumorigenesis.<sup>9</sup> Frequently co-amplified with *CDK4* is *CENTG1*. *CENTG1* encodes a GTPase called PIKE, which directly binds and activates PI 3-kinase and Akt.<sup>10-13</sup> PIKE-A, a member of the PIKE family, is present in various tissues with higher expression levels in the brain, spleen, thymus, small intestine and peripheral blood leukocytes.<sup>14-16</sup> PIKE-A contains the GTPase, PH, ArfGAP and two Ankyrin repeat domains present in PIKE-L, but lacks the N-terminal proline-rich domain, which binds protein 4.1N, PI 3-kinase and PLC-1.<sup>10,11</sup> PIKE-A directly binds to Akt and upregulates its activity in a GTP-dependent manner, mediating cancer cell invasion.<sup>12,13</sup> Human cancer cells with PIKE-amplification are more resistant to apoptosis compared with cancer cells with a normal PIKE-A copy number. Over-expression of wild-type PIKE-A has been shown to stimulate Akt activity and inhibit apoptosis, whereas it has been demonstrated that knockdown of PIKE-A diminishes Akt activity and enhances apoptosis. Therefore, PIKE-A amplification promotes cancer cell growth by inhibiting apoptosis through stimulation of Akt.<sup>12,13</sup> Moreover, PIKE-A acts as a proto-oncogene, promoting cancer cell survival, invasion and transformation through Akt activation.<sup>17</sup> Most recently, an automated network-based approach, which is used for determining candidate oncogenic processes and driver genes, identified new candidate cancer-causing drivers in GBM, including *AGAP2/CENTG1*, a putative oncogene and an activator of the PI 3-kinase pathway.<sup>18</sup> This approach is based on the hypothesis that cellular networks contain functional modules and that tumors target-specific modules critical to their growth. Thus, *CDK4* and *CENTG1* might comprise a functionally integrated oncogene DNA cluster that promotes aggressiveness in human cancers by cooperatively targeting the Rb1 and PI3K/AKT pathways.<sup>19</sup> In this report, we demonstrate that disruption of PIKE-A/Akt protein/protein interaction (PPI) leads to reduction of GBM cell proliferation, survival, migration and invasion. Moreover, peptides that inhibit this protein complex also sensitize GBM cells to two clinical anti-cancer medicines TMZ and Carmustine (BCNU), especially in GBM cells that harbor the *CDK4* amplicon. Therefore, our study provides a proof-of-concept that blockade of critical PPIs in GMB can be a therapeutic target for treating these devastating cancers.

## RESULTS

### PIKE-A interacts with Akt in live cells

We have previously demonstrated that PIKE-A interacts with Akt in human cancer cells, and determined that the N-terminus of PIKE-A and C-terminus of Akt regulate the interaction between these two proteins.<sup>12,13</sup> A schematic representation of the protein domains of PIKE-A and Akt and their binding motifs are shown in Figure 1a. Upon further mapping analysis, we found that the purified GST-tagged recombinant N-terminal fragment (a.a. 72-128) of PIKE-A interacted with HA-Akt (Figure 1b), which was independent with GTP/GDP.<sup>12</sup> To visualize the interaction between these two proteins, we utilized a Venus-based protein complementation assay. In this assay, the N-terminus of the Venus protein is

fused to one protein of interest, while the C-terminus of Venus is fused to another protein. If the two proteins bind to each other, the N-Venus and C-Venus proteins will come in close proximity allowing the Venus protein to reconstitute and yield a fluorescent signal after excitation. As 14-3-3 often exists as dimers, we used a 14-3-3 protein pair as a positive control. As expected, co-transfection of N-Venus-14-3-3 and C-Venus-14-3-3 resulted in a strong Venus signal, thereby validating this assay. To investigate whether the PIKE-A/Akt interaction occurred in cells, we sub cloned PIKE-A and Akt into pDEST26-C-Venus and pSCM167-N-Venus<sup>20</sup> vectors, respectively, and co-transfected these vectors into the LN229 GBM cell line. Similar to the 14-3-3 pair, co-expression of PIKE-A and Akt resulted in a robust Venus signal. In contrast, co-transfection of C-Venus-PIKE-A and the empty N-Venus vector or C-Venus-Akt and the empty C-Venus vector did not yield significant Venus signals (Figure 1c). Quantitative analysis of the resulting Venus signals is summarized in Figure 1d. Taken together, these results demonstrate that PIKE-A and Akt interact with each other in live LN229 cells.

### **Synthetic peptides (sp) derived from the binding motifs of PIKE-A and Akt block their interaction**

Although the whole protein X-ray structure of PIKE-A is not available yet, the three-dimensional structures of its GTPase domain and PH domain have been elucidated.<sup>21,22</sup> Molecular modeling of the N-terminus of PIKE-A (a.a. 1–128) predicts the protein folding to include several  $\alpha$ -strands, a  $\beta$ -helix and a loop (Figure 2a). Based on the predicted structure, we synthesized three peptides with 19 to 27 amino-acid residues (PP1 to PP3). To investigate whether these peptides could disrupt the interaction between PIKE-A and Akt, we conducted an *in vitro* binding assay using purified recombinant GST-PIKE-A protein and HA-Akt, which was isolated from transfected HEK293 cells. Introduction of PP1 or PP2 peptides into the binding solution completely disrupted the association between PIKE-A and Akt at both 10 and 50  $\mu$ M concentrations (Figure 2b).

The three-dimensional structure of Akt has been previously reported before.<sup>23</sup> As we have previously demonstrated that the C-terminus of Akt is required for its interaction with PIKE-A, we designed several small peptides (AP1-AP3) based on the C-terminal regulatory domain structure, which contains  $\alpha$ -helices and a loop structure (Figure 2c). Two of the small peptides, AP1 and AP3, robustly abolished the binding between PIKE-A and Akt, whereas AP2 enhanced the association between these two proteins in a dose-dependent manner (Figure 2d). To measure the affinity of interaction between PIKE-A and Akt, we examined the effect of various peptides on the interaction of the purified full-length PIKE-A and Akt in an *in vitro* binding assay. We found that PP1, PP2, AP1 and AP2 suppressed the interaction between PIKE-A and Akt in a concentration-dependent manner, with IC<sub>50</sub> of 0.41, 1.22, 0.87 and 14.06  $\mu$ M (Figure 2e). Furthermore, we evaluated the effect of candidate peptides by co-transfecting GST-PIKE-A and HA-Akt into HEK293 cells, followed by a GST pull-down assay performed in the presence of various antagonist peptides. Notably, incubation with PP1 resulted in the dose-dependent disruption of the PIKE-A/Akt interaction, which was also observed to a lesser degree upon incubation with AP1 and AP3. Interestingly, PP2 did not demonstrate an inhibitory effect, even at the 10  $\mu$ M concentration (Figure 2f). The discrepant efficacy of ability of the small peptides to inhibit the interaction between PIKE-A and Akt might result from the different folding conformations between full-length PIKE-A and the shorter form of PIKE-A (a.a. 1–356).

### **PP1 and AP1 disrupt the PIKE-A/Akt interaction in live cells**

To examine dissociating PIKE-A from Akt by the peptides in intact cells, we co-transfected N-Venus-PIKE-A and C-Venus-Akt into LN229 cells along with various GST-tagged antagonist peptides. As shown in Figure 3a, expression of GST-PP1 almost completely

blocked the binding between PIKE-A and Akt, whereas GST-PP2 and GST-AP1 partially reduced the association (Figure 3a). Quantitative analysis of the signals indicated that GST-PP1 and GST-AP1 significantly decreased the interaction between PIKE-A and Akt (Figure 3b). The expression of the transfected peptides, PIKE-A, and Akt were similar between all samples (Figure 3c).

### PP1 and AP1 suppress GBM cell survival, viability, migration and invasion

To investigate the biological effects of the PIKE-A/Akt interaction in GBM cells with different genetic backgrounds, we utilized the LN229 and LN-Z308 cell lines. Although LN229 cells do not contain the CDK4 amplicon, LN-Z308 cells possess the CDK4 amplicon.<sup>13</sup> After confirming the transfection efficiency (Supplementary Figure 1), we carried out tumorigenesis assays to evaluate the effect of peptides on GBM cell viability, migration and invasion. Transfection of GST-PP1 substantially reduced the survival of LN-Z308, whereas it had no effect on LN229 cells. Conversely, GST-AP1 significantly decreased the survival of LN229 cells, while it had negligible effect on LN-Z308 cells. The transfection efficiency was confirmed using co-transfected GFP (Supplementary Figure 1). As expected, GST and GST-PP2 did not have any effect on cell survival, regardless of the cell line (Figure 4a). Therefore, disrupting the interaction between PIKE-A and Akt strongly induces CDK4 amplicon-containing LN-Z308 cell death. Similar results were obtained from colony formation assays. GST-PP1 and GST-AP1 potently inhibited colony formation in LN-Z308 cells, while GST-AP1 significantly inhibited colony formation in LN229 cells (Figure 4b). TMZ and BCNU are two anti-cancer drugs that are used in the clinic for treatment of GBM. To test whether disrupting the PIKE-A/Akt interaction will further enhance the anti-cancer effects of these two drugs, we transfected LN229 and LN-Z308 cells with the short antagonist peptides and incubated the cells in the presence of 25  $\mu$ M of TMZ or 50- $\mu$ M BCNU. In LN229 cells, BCNU treatment reduced cell viability regardless of peptide transfection. However, in TMZ-treated cells, the PP1 peptide markedly reduced cell viability compared with the GST control and PP2 peptide. Although, TMZ treatment resulted in a modest effect in repressing LN229 cell viability compared with vehicle (Figure 4c). In LN-Z308 cells, transfection of PP1 or AP1 alone was sufficient to diminish cell viability. Interestingly, treatment with BCNU or TMZ did not prominently enhance effect of these peptides on cell viability (Figure 4d).

To examine the effect of disruption of the PIKE-A/Akt interaction on GBM on cell migration, we transfected the antagonist peptides into LN229 and LN-Z308 cells followed by cell migration analysis. The results demonstrated that none of these peptides significantly reduced the migration of LN229 cells. In contrast, both PP1 and AP1, but not PP2, potently reduced the migration of LN-Z308 cells as compared with control GST (Figure 4e). Moreover, we also investigated the effect of the peptides on GBM cell invasion. To this end, we co-transfected GST-tagged peptides with GFP into the GBM cells and quantitatively analyzed the invasion of GFP-positive cells. Both PP1 and AP1, but not PP2, robustly repressed the invasion of both LN229 and LN-Z308 cells as compared with control GST (Figure 4f). Collectively, these data suggest that inhibition of the PIKE-A/Akt PPI by the PP1 and AP1 peptides might suppress GBM cancer progression. Furthermore, we found that these peptides can also enhance the anti-cancer activities of TMZ and BCNU in CDK4 amplicon-containing GBM cells.

### Design of smaller synthetic peptides disrupting the PIKE-A/Akt interaction

The PP1, PP2 and AP1 peptides contain 19, 19 and 21 amino-acid residues, respectively. Owing to their relatively large size, they cannot penetrate the cell plasma membrane and enter live cells by diffusion. In order to develop smaller peptides that are able to enter live cells and disrupt the PIKE-A/Akt interaction, we synthesized three shorter peptides for each

of the above peptides. The sequence of each of the short peptides is listed in Figure 5a. The results from an *in vitro* binding assay revealed that the sp2 peptide (PELRLGVL) from PP1, sp4 peptide (DARSG) and sp6 peptide (TGSYQ) from PP2, and sp9 peptide (LKKDPK) from AP1 decreased the interaction between a fragment of PIKE-A (1–356 a.a.) and Akt (Figures 5a and b). Quantitative analysis of several independent assays indicated that at 50  $\mu$ M sp2, sp4 and sp6 significantly disrupt the interaction between PIKE-A and Akt. Notably, at 10  $\mu$ M, PP2 and smaller peptides derived from PP2, sp4 and sp6, failed to block the PIKE-A/Akt interaction, but at 50  $\mu$ M, sp4 and sp6 peptides were able to disrupt the interaction between PIKE-A and Akt (Figure 5c). To further investigate the inhibitory effects of the shorter peptides, we co-transfected GST-PIKE-A full-length and HA-Akt and performed GST pull-down assay. The results from these assays indicate that sp2, sp4 and sp6 exhibit a dose-dependent reduction of the binding of PIKE-A to Akt; in contrast, none of the short peptides from the Akt C-terminal peptide, AP1, exhibited an inhibitory effect (Figure 5d). As expected, the longer peptide PP1 displayed a slightly more potent inhibitory effect on the PIKE-A/Akt interaction than sp2, whereas the sp5 peptide had no effect at all (Figure 5e). To assess whether the small peptide sp2 could disrupt the PIKE-A/Akt complex in a time dependent manner, we co-transfected HEK293 cells with GST-PIKE-A and HA-Akt, then treated the cells with 50- $\mu$ M sp2 for various time points and conducted a GST pull-down assay. The sp2 peptide inhibited PIKE-A binding to Akt at 4 h. The inhibition increased in a time-dependent manner and peaked at 16 h. At 24 h, the peptide lost its suppressive activity (Figure 5f). Presumably, this peptide was degraded after 24-h incubation in cell culture medium.

### sp2 inhibits GBM cell viability, migration, invasion and colony formation

We next sought to determine the effect of these smaller peptides on GBM cell survival, migration, invasion and colony formation. To this end, we treated LN229 and LN-Z308 cells with 50  $\mu$ M of the various small antagonistic peptides. The results from an MTT assay demonstrated that sp2 and sp6 selectively decreased LN-Z308 cell viability, whereas sp4 had no effect. Interestingly, the reduction in viability caused by the sp2 and sp6 peptides was only observed in LN-Z308 cells, not in LN229 cells (Figure 6a). Similar results were seen in cell migration assays (Figure 6b). Conversely, sp2 strongly inhibited the invasive activity of both LN229 and LN-Z308 cells. Notably, sp4 and sp6 did not significantly affect in invasive activity of either cell line (Figure 6c). To determine whether the sp2 peptide acted additively or synergistically with commonly used anti-cancer drugs on GBM cell viability, we treated LN229 and LN-Z308 cells with TMZ (25  $\mu$ M) or BCNU (50  $\mu$ M) in the presence of various concentration of sp2. The results from these assays revealed a suppressive activity of sp2 on LN-Z308 cell viability, which occurred in a dose-dependent manner. However, its activity towards LN229 cells was not as evident as in LN-Z308 cells. TMZ potentially decreased both LN-Z308 and LN229 cell viability and co-treatment with the sp2 peptide elicited an additive effect in LN-Z308 cells. The inhibitory trend was similar in LN229 cells. Similar results on cell viability were observed for co-treatment of sp2 peptide and BCNU (Figure 6d). To assess the effect of sp2 on the colony formation inhibitory effects of TMZ and BCNU, we treated GBM cells lines with TMZ or BCNU in the presence of various doses of sp2. The results from the colony formation assays revealed that TMZ and BCNU decreased the colony numbers of both cells. This effect was substantially increased by co-treatment with 50- $\mu$ M sp2 in LN-Z308 cells. The additive trend also applied in LN229 cells (Figure 6e). Furthermore, similar observations were observed in TP366 cells, another CDK4 amplicon-expressing GBM cell line (Data not shown). Taken together, these results indicate that a small peptide from the PIKE-A N-terminus, sp2, can potentially suppress brain cancer cell viability, migration and invasion. Moreover, we have demonstrated that CDK4 amplicon-containing cells are more sensitive to treatment with sp2.

### sp2 inhibits the endogenous interaction between PIKE-A and Akt

Our studies indicate that sp2 strongly inhibits LN-Z308 cell viability, migration, invasion and colony formation. This suppressive activity may occur through the ability of sp2 to disrupt the PIKE-A/Akt interaction, leading to blockade of signaling cascades downstream of Akt. To investigate this possibility, we treated LN-Z308 cells with different concentrations of sp2 peptide, or sp4 peptide as a control. Co-immunoprecipitate assays demonstrated that sp2 disrupts the association between endogenous PIKE-A/Akt in a dose-dependent manner, whereas SP4 did not affect the PIKE-A/Akt interaction (Figure 7a). Our previous studies demonstrate that PIKE-A is required for Akt activation.<sup>12,24</sup> Immunoblotting analysis of peptide-treated cell lysates indicates that both Akt T308 and S473 phosphorylation were diminished by sp2 peptide treatment in a dose-dependent manner, whereas SP4 had no effect on Akt phosphorylation. These results support the hypothesis that abolishment of the PIKE-A/Akt association leads to a reduction in Akt activity. In agreement with these observations, the well-established downstream effectors of Akt including mTOR, rpS6 and GSK3a exhibited the similar decreased phosphorylation patterns after treatment with sp2 (Figure 7b). Collectively, these results indicate that disruption of the PIKE-A/Akt interaction by the sp2 peptide decreases Akt activation and thus signaling cascades downstream of Akt.

## DISCUSSION

The key finding of this report is that disruption of the PIKE-A/Akt interaction in GBM cells by small antagonist peptides decreases cell viability, suppresses cell migration and invasion, diminishes colony formation and additively enhances the effects of the commonly used chemotherapeutic drugs. Moreover, we found that CDK4 amplicon-containing GBM cells are more sensitive to the effects of the small peptides than the GBM cells without the CDK4 amplicon. Our previous studies established that a pronounced overexpression of PIKE-A in a variety of human tumors and that the activation of Akt by PIKE-A contributed to the progression of these tumors.<sup>12,13,17</sup> In the current report, we provide compelling evidence to demonstrate that inhibition of the interaction between PIKE-A and Akt substantially blocks GBM cell viability, migration, invasion and colony formation. The small peptides we identified from the N-terminus of PIKE-A provided us with a powerful tool to specifically interrogate the biological actions of the PIKE-A/Akt interaction in cancer cell development. The small peptide sp2 contains only 8 amino acids with molecular weight about 878.1 U. This peptide effectively disrupts the endogenous PIKE-A/Akt associate in GBM cells, resulting in the suppression of Akt signaling cascades. Our results indicate that sp2 might be able to penetrate intact cells and exert its inhibitory effects by blocking the interaction between PIKE-A and Akt.

PI 3-kinase/Akt signaling cascade is commonly activated in many human malignancies, including GBM. This pathway can be activated via numerous upstream alterations including genomic amplification of epidermal growth factor receptor, PTEN deletion or PIK3CA mutations. Akt promotes cell survival by inhibiting proteins that mediate apoptosis and by upregulating proteins that inhibit apoptosis. For example, Akt phosphorylates the pro-apoptotic Bcl-2 family member BAD,<sup>25,26</sup> caspase-9<sup>27</sup> and apoptosis signal-regulating kinase 1 (Ask1)<sup>28</sup> and inhibits their pro-apoptotic functions. In addition, Akt is a crucial factor in regulating diverse tumorigenic activities such as angiogenesis and tissue invasion/metastasis.<sup>29</sup> Inhibition of PI 3-kinase/Akt signaling has been well characterized as a therapeutic target for treating various human cancers including GBM. Nonetheless, Akt is essential for a variety of molecular and cellular processes in normal cells. Direct blockade of Akt might disturb numerous ordinary cellular processes and yield undesirable side effects. The feasibility of targeting PPIs for functional studies has been well established. As an increasing number of protein complexes and interconnected protein networks are revealed

by a variety of experimental approaches, general principles underlying PPIs and their roles in controlling cellular processes have emerged. It appears that a general mode of PPI is mediated by a contiguous stretch of amino-acid sequences or a defined structure to form protein domains or modules within individual proteins.<sup>30</sup> These protein domains or modules offer tractable molecular targets for tool design and mechanistic interventions. For example, molecular studies have mapped the MDM2/p53 interaction interfaces to a 15-residue - helical region of p53, which has been extensively targeted for defining the oncogenic properties of MDM2 in a number of tumors, including GBM. Thus, using a peptide disruption approach is expected to identify critical PPIs in oncogenic signaling pathways in GBM. The exciting data presented in this report provide a proof-of-concept that targeting a crucial PPI in GBM may not only address its biological roles in cancer progression but also establish a drug-screening target for cancer treatment. Here, we provide an alternative approach to target Akt activation by disrupting the PIKE-A/Akt interaction. Conceivably, targeting this PPI, instead of inhibiting Akt itself directly, might result in less severe side effects. The small peptides identified in this study could be used as a template for *in silico* screening to search for small molecules that may share a similar three-dimensional structure as the 8-mer peptide, and thus specifically abolish the interaction between PIKE-A and Akt. Conversely, the fluorescent live-cell image analysis could be used as a screening tool to quantitatively screen small molecules to inhibit the PIKE-A/Akt interaction. The compounds that are discovered through these studies may serve as positive hits for further drug development for the treatment of cancer.

In the present study, we have found that GBM cells that harbor the CDK4 amplicon are more responsive to dissociation of the PIKE-A/Akt interaction than GBM cells without the CDK4 amplicon (Figures 4 and 6). CDK4 amplicon contains *CDK4*, *CENTG1*, *SAS* and *OS9* genes. This amplicon is frequently amplified in numerous human cancers including sarcoma, brain tumors, lung cancer, melanoma and so on.<sup>3-7</sup> It often co-amplifies with the oncogene MDM2. Presumably, these oncogenes coordinate with each other to upregulate proliferative signals and enhance cancer cell growth and transformation. In addition, Cdks have essential roles in regulating cell proliferation and tumorigenesis. During the G<sub>1</sub> phase, Rb proteins are inactivated by sequential phosphorylation mediated by various Cdks, mainly the D-type cyclin-dependent Cdk4 and Cdk6 and the E-type cyclin-dependent Cdk2.<sup>31</sup> Inactivation of Rb proteins results in the release and/or activation of proteins, including E2F, required for cell cycle progression. Conceivably, GBM cells with the CDK4 amplicon might be more dependent on CDK4 and PIKE-A proteins to gain extra proliferation advantage. The concomitant contribution of CDK4 and PIKE-A/Akt signaling to tumor progression might provide a selective target for future personalized anti-cancer drug therapy. Taken together, our study demonstrates the interrogation of a PPI in GBM using small peptides can provide the biological roles of PPIs in cancer progression, which lays down the groundwork for subsequent investigation of the PPI's functions in tumorigenesis in animal models. This knowledge paves the way for targeting the specific PPI for further drug screening and development.

## MATERIALS AND METHODS

### Cell lines and reagents

HEK293 cells and the human glioblastoma, LN229, LN-Z308 and TP366 cells were maintained in DMEM with 10% FBS and 1X pen/strep/glutamine supplemented with various selection antibiotics at 37 °C in a 5% CO<sub>2</sub> atmosphere in a humidified incubator. Anti-HA-HRP and anti-GST-HRP antibodies were from Sigma (St Louis, MO, USA). All other antibodies were from Cell Signaling (Beverly, MA, USA). The Horseradish peroxidase linked IgG secondary antibodies were purchased from GE healthcare (Sweden, UK). Protein A/G-conjugated agarose beads were from Calbiochem (Darmstadt, Germany).

Glutathione Sepharose 4B was supplied by Amersham Pharmacia (Sweden, UK). All of the chemicals not included above were from Sigma.

### Plasmid construction

All plasmids were constructed using Gateway technology (Invitrogen, Carlsbad, CA, USA) according to the manufacturer's protocols. The pDEST26-C-Venus (Invitrogen) and pSCM167-N-Venus<sup>20</sup> vectors were used as vectors. Insertions were amplified by PCR and then inserted into the pDONR201 vector using a BP reaction. An LR reaction was used to transfer the desired DNA into the appropriate destination vectors. All constructs were verified by sequencing analysis.

### Cell viability assay

Cells were seeded in 96-well plates at a density of 3000 cells per well. The next day, the medium was replaced with fresh medium containing drugs/peptides or vehicle controls. Cells were incubated at 37 °C for indicated times. The cell proliferation was monitored by an MTT/BrdU incorporation assay according to the manufacturer's protocols.

### Cell migration and invasion assays

Cells (300 000 per well) were seeded in a six-well plate. Approximately 24 h later, when the cells were 100% confluent, the monolayer was scratched using a 200- $\mu$ l pipette tip and washed once to remove nonadherent cells. New medium containing the antagonist peptides or DMSO was added (0 h) and allowed to incubate for 10 h. The cells were observed using a light microscope. Inhibition of migration was assessed using Image J software, available from the National Institutes of Health Web site (<http://rsb.info.nih.gov/ij/>). The percent of wound healed was calculated using the formula:  $100 - [(final\ area/initial\ area) \times 100\%]$ . For cell invasion assay, invasion of cells through Matrigel was determined using a transwell system (10 mm diameter, 8  $\mu$ m pore size with polycarbonate membrane; Corning Costar) as described previously.<sup>17</sup>

### Colony formation assay

A base 0.6% agar gel with 10% FBS in DMEM was prepared and added to the wells of a six-well culture dish. Cells were plated at a density of 50 000 cells per well on top of the base agar for anchorage-independent growth analysis in 0.4% agar gel with 10% FBS in DMEM supplemented with drugs/peptides or vehicle. The cells were maintained at 37 °C and allowed to grow for 2 weeks. The colonies were stained using MTT dye (100  $\mu$ l per well). The colonies were scored and the numbers were normalized as the percentage of colonies formed in vehicle.

### Co-immunoprecipitation and *in vitro* binding assays

Experimental procedures for the co-immunoprecipitation and *in vitro* binding assays have been previously described.<sup>32</sup>

### ELISA protein interaction assay

Reacti-Bind glutathione-coated ELISA plates (Pierce, Rockford, IL, USA) were treated with purified GST-PIKE-A (a.a. 1 - 356) for 16 h at 4 °C and then washed three times with wash buffer (10 mM Tris-HCl, pH 7.4, 150 mM NaCl, 0.05% Tween-20). Peptides were added to the wells (20  $\mu$ l/well) and incubated for 3 h at room temperature, followed by incubation with HA-Akt-containing cytosolic extracts from transfected HEK293 cells diluted in wash buffer for 4 h at room temperature. Akt binding was detected with biotin-conjugated Akt antibody and streptavidin-horseradish peroxidase (0.5 mg/ml; Jackson ImmunoResearch, West Grove, PA, USA). Color development was stopped after 1 - 2 min by the addition of



100  $\mu$ l of 0.2-M citric acid/well. OD405- 490 was quantitated on a 96-well plate reader (Synergy 2, Bioteck, Winooski, VT, USA).

### Statistical analysis

Data are presented as mean $\pm$ s.d. of three or four independent experiments. Statistical evaluation was carried out using the Student's *t*-test. Data were considered statistically significant when  $P < 0.05$ . All statistical analyses were performed using Prism GraphPad software (La Jolla, CA, USA).

### Supplementary Material

Refer to Web version on PubMed Central for supplementary material.

### Acknowledgments

This work is supported by federal funds from the National Cancer Institute, National Institutes of Health, under Contract No. HHSN261200800001E (H Fu) and RO1 CA127119 (K Ye). The content of this publication does not necessarily reflect the views or policies of the Department of Health and Human Services, nor does mention of trade names, commercial products, or organizations imply endorsement by the US Government.

### References

1. Grzmil M, Hemmings BA. Deregulated signalling networks in human brain tumours. *Biochem Biophys Acta*. 2010; 1804:476–483. [PubMed: 19879382]
2. Stupp R, Mason WP, van den Bent MJ, Weller M, Fisher B, Taphoorn MJ, et al. Radiotherapy plus concomitant and adjuvant temozolomide for glioblastoma. *N Engl J Med*. 2005; 352:987–996. [PubMed: 15758009]
3. Khatib ZA, Matsushime H, Valentine M, Shapiro DN, Sherr CJ, Look AT. Coamplification of the CDK4 gene with MDM2 and GLI in human sarcomas. *Cancer Res*. 1993; 53:5535–5541. [PubMed: 8221695]
4. Reifenberger G, Reifenberger J, Ichimura K, Meltzer PS, Collins VP. Amplification of multiple genes from chromosomal region 12q13-14 in human malignant gliomas: preliminary mapping of the amplicons shows preferential involvement of CDK4, SAS, and MDM2. *Cancer Res*. 1994; 54:4299–4303. [PubMed: 8044775]
5. Reifenberger G, Ichimura K, Reifenberger J, Elkahoul AG, Meltzer PS, Collins VP. Refined mapping of 12q13-q15 amplicons in human malignant gliomas suggests CDK4/SAS and MDM2 as independent amplification targets. *Cancer Res*. 1996; 56:5141–5145. [PubMed: 8912848]
6. Wikman H, Nymark P, Vayrynen A, Jarmalaite S, Kallioniemi A, Salmenkivi K, et al. CDK4 is a probable target gene in a novel amplicon at 12q13.3-q14.1 in lung cancer. *Genes Chromosomes Cancer*. 2005; 42:193–199. [PubMed: 15543620]
7. Muthusamy V, Hobbs C, Nogueira C, Cordon-Cardo C, McKee PH, Chin L, et al. Amplification of CDK4 and MDM2 in malignant melanoma. *Genes Chromosomes Cancer*. 2006; 45:447–454. [PubMed: 16419059]
8. Sherr CJ, Roberts JM. Living with or without cyclins and cyclin-dependent kinases. *Genes Dev*. 2004; 18:2699–2711. [PubMed: 15545627]
9. Miliani de Marval PL, Macias E, Conti CJ, Rodriguez-Puebla ML. Enhanced malignant tumorigenesis in Cdk4 transgenic mice. *Oncogene*. 2004; 23:1863–1873. [PubMed: 14647432]
10. Ye K, Hurt KJ, Wu FY, Fang M, Luo HR, Hong JJ, et al. Pike. A nuclear gtpase that enhances PI3kinase activity and is regulated by protein 4. *IN. Cell*. 2000; 103:919–930. [PubMed: 11136977]
11. Ye K, Aghdasi B, Luo HR, Moriarity JL, Wu FY, Hong JJ, et al. Phospholipase C gamma 1 is a physiological guanine nucleotide exchange factor for the nuclear GTPase PIKE. *Nature*. 2002; 415:541–544. [PubMed: 11823862]

12. Ahn JY, Hu Y, Kroll TG, Allard P, Ye K. PIKE-A is amplified in human cancers and prevents apoptosis by up-regulating Akt. *Proc Natl Acad Sci USA*. 2004; 101:6993–6998. [PubMed: 15118108]
13. Ahn JY, Rong R, Kroll TG, Van Meir EG, Snyder SH, Ye K. PIKE (phosphatidylinositol 3-kinase enhancer)-A GTPase stimulates Akt activity and mediates cellular invasion. *J Biol Chem*. 2004; 279:16441–16451. [PubMed: 14761976]
14. Nagase T, Seki N, Ishikawa K, Tanaka A, Nomura N. Prediction of the coding sequences of unidentified human genes. V. The coding sequences of 40 new genes (KIAA0161-KIAA0200) deduced by analysis of cDNA clones from human cell line KG-1. *DNA Res*. 1996; 3:17–24. [PubMed: 8724849]
15. Xia C, Ma W, Stafford LJ, Liu C, Gong L, Martin JF, et al. GGAPs, a new family of bifunctional GTP-binding and GTPase-activating proteins. *Mol Cell Biol*. 2003; 23:2476–2488. [PubMed: 12640130]
16. Elkahloun AG, Krizman DB, Wang Z, Hofmann TA, Roe B, Meltzer PS. Transcript mapping in a 46-kb sequenced region at the core of 12q13. 3 amplification in human cancers. *Genomics*. 1997; 42:295–301. [PubMed: 9192850]
17. Liu X, Hu Y, Hao C, Rempel SA, Ye K. PIKE-A is a proto-oncogene promoting cell growth, transformation and invasion. *Oncogene*. 2007; 26:4918–4927. [PubMed: 17297440]
18. Cerami E, Demir E, Schultz N, Taylor BS, Sander C. Automated network analysis identifies core pathways in glioblastoma. *PLoS One*. 2010; 5:e8918. [PubMed: 20169195]
19. Kim H, Huang W, Jiang X, Pennicooke B, Park PJ, Johnson MD. Integrative genome analysis reveals an oncomir/oncogene cluster regulating glioblastoma survivor-ship. *Proc Natl Acad Sci USA*. 2010; 107:2183–2188. [PubMed: 20080666]
20. Min W, Lin Y, Tang S, Yu L, Zhang H, Wan T, et al. AIP1 recruits phosphatase PP2A to ASK1 in tumor necrosis factor-induced ASK1-JNK activation. *Circ Res*. 2008; 102:840–848. [PubMed: 18292600]
21. Soundararajan M, Yang X, Elkins JM, Sobott F, Doyle DA. The centaurin gamma-1 GTPase-like domain functions as an NTPase. *Biochem J*. 2007; 401:679–688. [PubMed: 17037982]
22. Yan J, Wen W, Chan LN, Zhang M. Split pleckstrin homology domain-mediated cytoplasmic-nuclear localization of PI3-kinase enhancer GTPase. *J Mol Biol*. 2008; 378:425–435. [PubMed: 18371979]
23. Kumar CC, Madison V. AKT crystal structure and AKT-specific inhibitors. *Oncogene*. 2005; 24:7493–7501. [PubMed: 16288296]
24. Chan CB, Liu X, He K, Qi Q, Jung DY, Kim JK, et al. The association of phosphoinositide 3-kinase enhancer A with hepatic insulin receptor enhances its kinase activity. *EMBO Rep*. 2011; 12:847–854. [PubMed: 21720388]
25. Datta SR, Dudek H, Tao X, Masters S, Fu H, Gotoh Y, et al. Akt phosphorylation of BAD couples survival signals to the cell-intrinsic death machinery. *Cell*. 1997; 91:231–241. [PubMed: 9346240]
26. del Peso L, Gonzalez-Garcia M, Page C, Herrera R, Nunez G. Interleukin-3-induced phosphorylation of BAD through the protein kinase Akt. *Science*. 1997; 278:687–689. [PubMed: 9381178]
27. Cardone MH, Roy N, Stennicke HR, Salvesen GS, Franke TF, Stanbridge E, et al. Regulation of cell death protease caspase-9 by phosphorylation. *Science*. 1998; 282:1318–1321. [PubMed: 9812896]
28. Kim AH, Khursigara G, Sun X, Franke TF, Chao MV. Akt phosphorylates and negatively regulates apoptosis signal-regulating kinase 1. *Mol Cell Biol*. 2001; 21:893–901. [PubMed: 11154276]
29. Testa JR, Bellacosa A. AKT plays a central role in tumorigenesis. *Proc Natl Acad Sci USA*. 2001; 98:10983–10985. [PubMed: 11572954]
30. Scott JD, Pawson T. Cell signaling in space and time: where proteins come together and when they're apart. *Science*. 2009; 326:1220–1224. [PubMed: 19965465]
31. Ortega S, Malumbres M, Barbacid M. Cyclin D-dependent kinases, INK4 inhibitors and cancer. *Biochem Biophys Acta*. 2002; 1602:73–87. [PubMed: 11960696]

32. Ye K, Compton DA, Lai MM, Walensky LD, Snyder SH. Protein 4. 1N binding to nuclear mitotic apparatus protein in PC12 cells mediates the antiproliferative actions of nerve growth factor. *J Neurosci.* 1999; 19:10747–10756. [PubMed: 10594058]

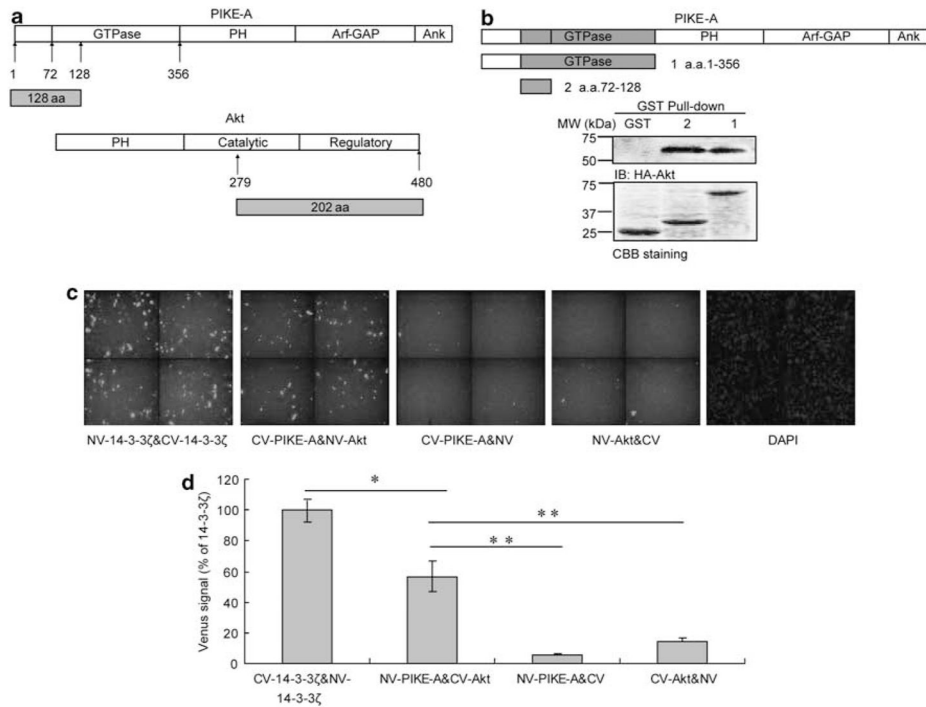


**Figure 1.** PIKE-A interacts with Akt *in vitro* and *in vivo*. (a) Diagram of the binding fragments of PIKE-A and Akt. (b) *In vitro* binding assay. HEK293 cells were transfected with hem agglutinin (HA)-tagged Akt. Purified recombinant GST-PIKE-A (a.a. 1–356) protein was conjugated to glutathione beads and incubated with 293 cell lysates at 4 °C for 3 h. The glutathione bead-associated proteins were resolved by 10% SDS-PAGE and analyzed by immunoblotting with an anti-HA antibody. GST-recombinant proteins were verified by Coomassie Brilliant Blue (CBB) staining. (c) PIKE-A binds to Akt in living cells. Protein complementation assays (PCA) were performed. LN229 cells (5000 cells/well) were seeded in a 96-well plate. Co-transfected C-Venus-PIKE-A and N-Venus-Akt interacted with each other in LN229 cells. Following 40 transfection, positive signals were quantified. The 14-3-3 homodimer was used as a positive control. (d) Quantification of the PCA signals in test and control groups. PCA signals were significantly increased compared with negative controls. Data represent mean±s.d. (\* $P<0.05$ , \*\* $P<0.01$ ).

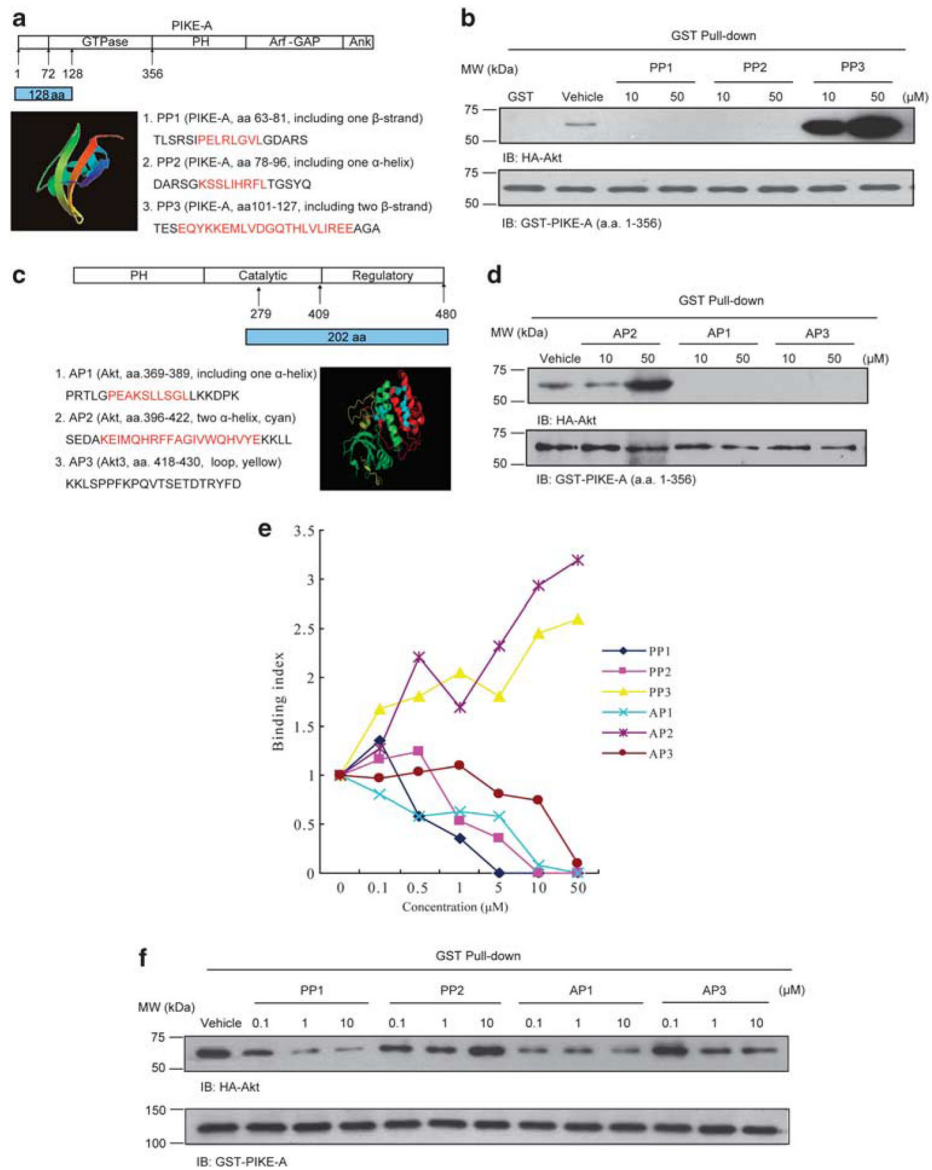


**Figure 2.** sp derived from the binding motifs of PIKE-A and Akt disrupt their association. **(a)** The sequences of PIKE-A-derived sp. Based on the structure predicted by the SWISS-MODEL database, candidate peptides from the interaction region of PIKE-A (a.a. 1–128) with Akt were designed. **(b)** *In vitro* binding assay as described in Figure 1. PP1 and PP2 inhibited the interaction between PIKE-A and Akt. **(c)** The sequences of Akt-derived sp. Based on the crystal structure of Akt, candidate peptides from the interaction region of Akt (a.a. 279–480) with PIKE-A were designed. **(d)** *In vitro* binding assay as described in Figure 1. AP1 and AP3 inhibited the interaction of PIKE-A and Akt in a dose-dependent manner. **(e)** PP1, PP2 and AP1 suppress the purified recombinant PIKE-A and Akt in a concentration-dependent manner. *In vitro* binding assay: 0.5  $\mu$ g of purified Akt were incubated with glutathione bead-associated GST-PIKE-A for over night in the presence of indicated concentrations of peptides. The glutathione bead-associated proteins were resolved on 10% SDS-PAGE and analyzed by immunoblotting with Akt antibody. Then the binding index was calculated after normalization with GST-PIKE-A using Image J software. **(f)** GST-pull down assay.

HEK293 cells were co-transfected with HA-Akt and GST-PIKE-A. After 40 h, the cell lysate was collected and GST-PIKE-A was pulled down with glutathione beads. The associated proteins were analyzed by immunoblotting with an anti-HA antibody. GST-PIKE-A was verified with anti-GST-HRP.

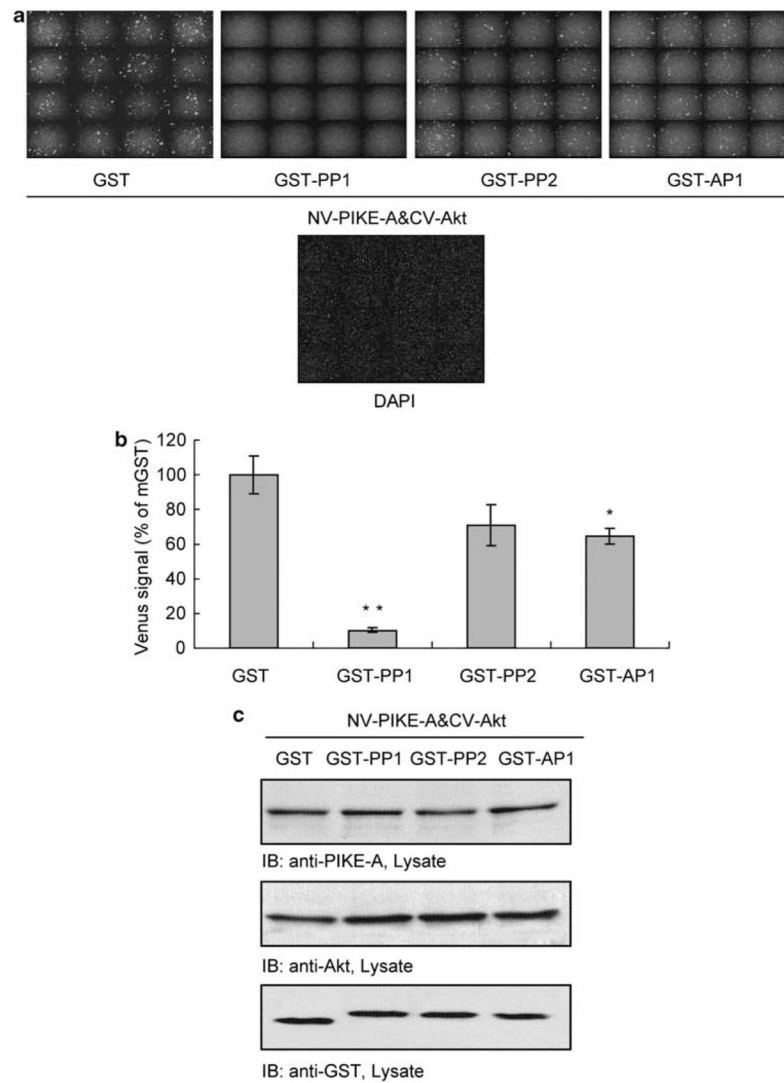


**Figure 3.** PP1 and AP1 disrupt the PIKE-A/Akt interaction in living cells. **(a)** PP1 and AP1 inhibit the binding of PIKE-A and Akt in LN229 cells. Peptides were placed into GST-tagged vectors using Gateway techniques. LN229 cells (5000 cells/well) were seeded in a 96-well plate. The peptide plasmids were co-transfected with the Venus plasmids. Following 40 transfection, positive signals were quantified. **(b)** Quantification of the PCA signals in test and control groups. PP1 and AP1 significantly decreased the PCA signals compare with control. Data represent mean±s.d. (\* $P$ <0.05, \*\* $P$ <0.01). **(c)** Expression of N-Venus-PIKE-A, C-Venus-Akt and the peptides used in the PCA system was verified by immunoblotting analysis with the indicated antibodies.

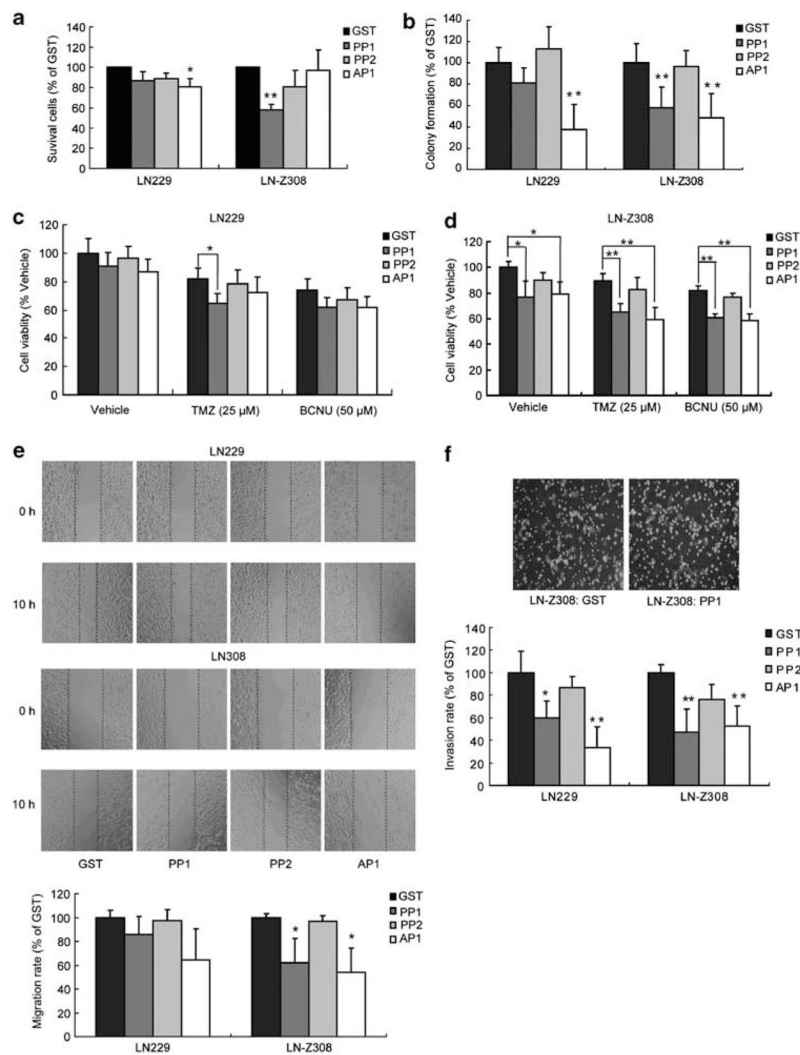


**Figure 4.** PP1 and AP1 suppress GBM cell survival, colony formation, migration and invasion. **(a)** Cell survival assay. Cells ( $1 \times 10^5$ /well) were seeded in six-well plates. FuGENE HD transfection reagent was used to transfect the cells with the peptides and vector plasmids. After 40 h, a trypan blue exclusion assay was utilized to measure the viability of cells transfected with the fusion peptide encoding plasmids. **(b)** Colony formation assay. The potency of peptides was assessed further in an anchorage-independent environment using a colony formation assay. Treatment with PP1 greatly decreased the ability of LN-Z308 cells to form colonies in comparison with GST control. **(c)** A cell viability assay (MTT) was conducted to determine the effect of the peptides and examine whether there was a synergetic effect with BCNU or TMZ in LN229 cells. Cells ( $5 \times 10^3$ /well) were seeded in 96-well plates followed by transfection with the indicated plasmid and vector. After 40 h, the medium was replaced with medium containing BCUN (50 μM) or TMZ (25 μM). Following 24 h of treatment, an MTT assay was employed to determine cell viability. **(d)** PP1 and AP1 inhibited cell viability in LN-Z308 cells. Combined treatment of PP1 or AP1 with BCNU or TMZ enhanced the inhibition of BCNU/TMZ in LN-Z308 cells by MTT assay as in **(c)**. **(e)** Cells ( $1 \times 10^5$ /well) were seeded in six-well plates. Peptides and vector plasmids were transfected with FuGENE HD transfection reagent. After 40 h, cell migration



was determined using a wound-healing assay. Mention the quantification/statistics used (f). Cells ( $1 \times 10^5$ /well) were seeded in six-well plates. Peptides, vector plasmids and GFP expression plasmids were transfected with FuGENE HD transfection reagent. After 40 h, cell invasion was determined using a transwell invasion assay as described. Data represent mean $\pm$ s.d. (\* $P < 0.05$ , \*\* $P < 0.01$ ).

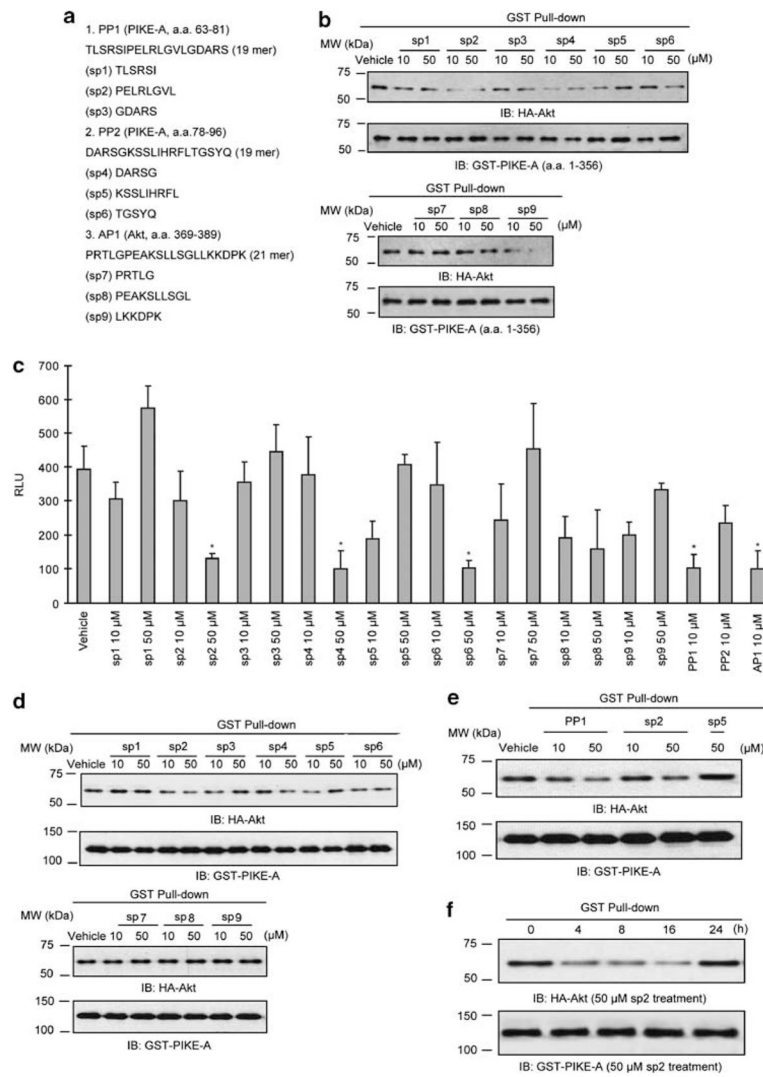


**Figure 5.** Comparison with the inhibition of PIKE-A/Akt binding by the small sp derived from PP1, PP2 and AP1. **(a)** Sequence and number of amino acids of the small sp. **(b)** *In vitro* binding assay as described in Figure 1. sp2, sp4, sp6 and sp9 inhibited the interaction of PIKE-A and Akt. **(c)** An ELISA-based protein interaction assay was used to verify the ability of the small peptides to inhibit PIKE-A and Akt binding. sp2, sp4 and sp6 significantly disrupted the interaction of PIKE-A and Akt. Data of RLU (relative luminescence units) represent mean  $\pm$  s.d. (\* $P$ <0.05, \*\* $P$ <0.01). **(d)** sp2 inhibited interaction of PIKE-A and Akt in living cells. HEK293 cells were co-transfected with HA-Akt and GST-PIKE-A, followed by treatment with indicated concentrations of the sps. GST-PIKE-A was pulled down with glutathione beads. The associated proteins were analyzed with an anti-HA antibody. GST-PIKE-A was verified with anti-GST-HRP. Sp2 suppressed the interaction of PIKE-A and Akt *in vivo*. **(e)** A GST-pull down assay as described in Figure 2 demonstrated that both PP1 and SP2 inhibited the binding of PIKE-A and Akt. **(f)** Time-course study of the effect of sp2 on the interaction of PIKE-A and Akt. HEK293 cells were co-transfected with HA-Akt and GST-PIKE-A, followed by treatment with sp2 (50 μM) for the indicated times. GST-PIKE-A was pulled down with glutathione beads. The associated proteins were analyzed with an anti-HA

antibody. Treatment with sp2 for 16 h significantly decreased the interaction of PIKE-A and Akt.

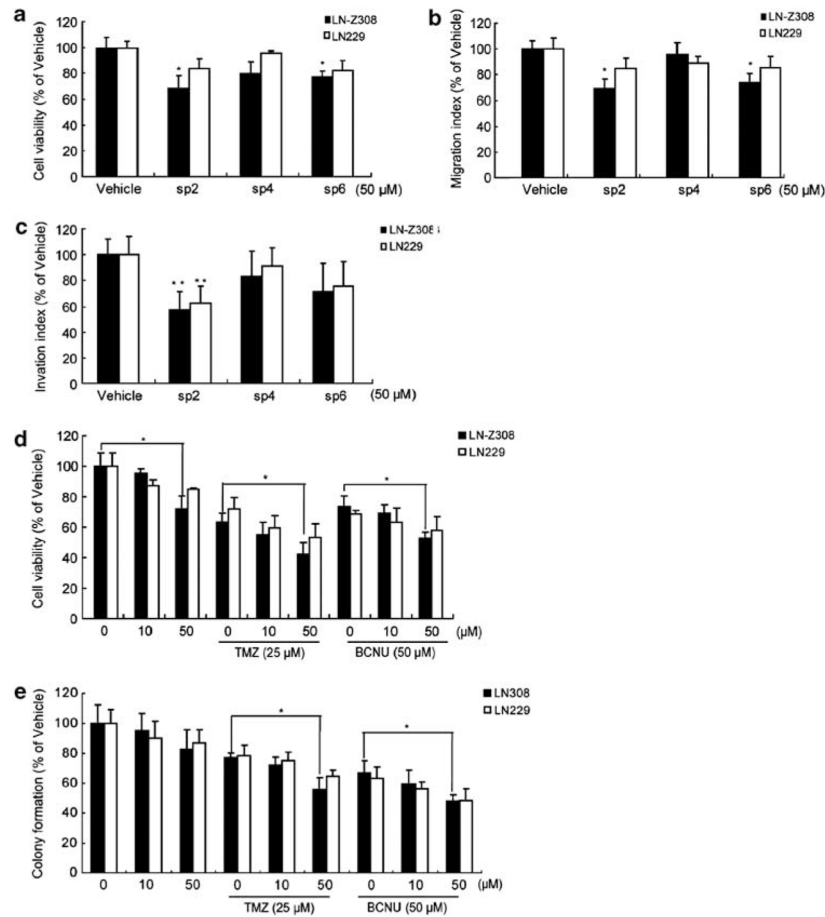


**Figure 6.**

sp2 inhibits GBM cell viability, migration, invasion and colony formation. **(a)** Cell viability assay. Cells ( $5 \times 10^3$ /well) were seeded in 96-well plates followed by treatment with the indicated peptides for 16 h. An MTT assay was performed to determine the effect of the sps on the viability of LN229 and LN-Z308 cells. **(b)** Cell migration assay. Cells ( $1 \times 10^5$ /well) were seeded in six-well plates, cell migration was studied using a healing assay in the presence of the indicated peptides. After 10 h, the migration image was collected and analyzed by Image J software. **(c)** Cell invasion assay. Cells ( $1 \times 10^5$ /well) were seeded in six-well plates followed by treatment with the indicated peptides 16 h. Cell invasion was determined using a transwell invasion assay described. **(d)** The effect of sp2 alone or in combination with BCNU or TMZ, on cell viability. Cells ( $5 \times 10^3$ /well) were seeded in 96-well plates followed by treatment with sp2 in the absence or presence of BCNU/TMZ at the indicated concentrations for 16 h. An MTT assay was performed to determine cell viability. **(e)** The effect of sp2 alone or in combination with BCNU or TMZ on colony formation. Combined treatment of sp2 enhanced the inhibitory effects of BCNU/TMZ on LN-Z308 colony formation. Data represent mean $\pm$ s.d. (\* $P < 0.05$ , \*\* $P < 0.01$ ).

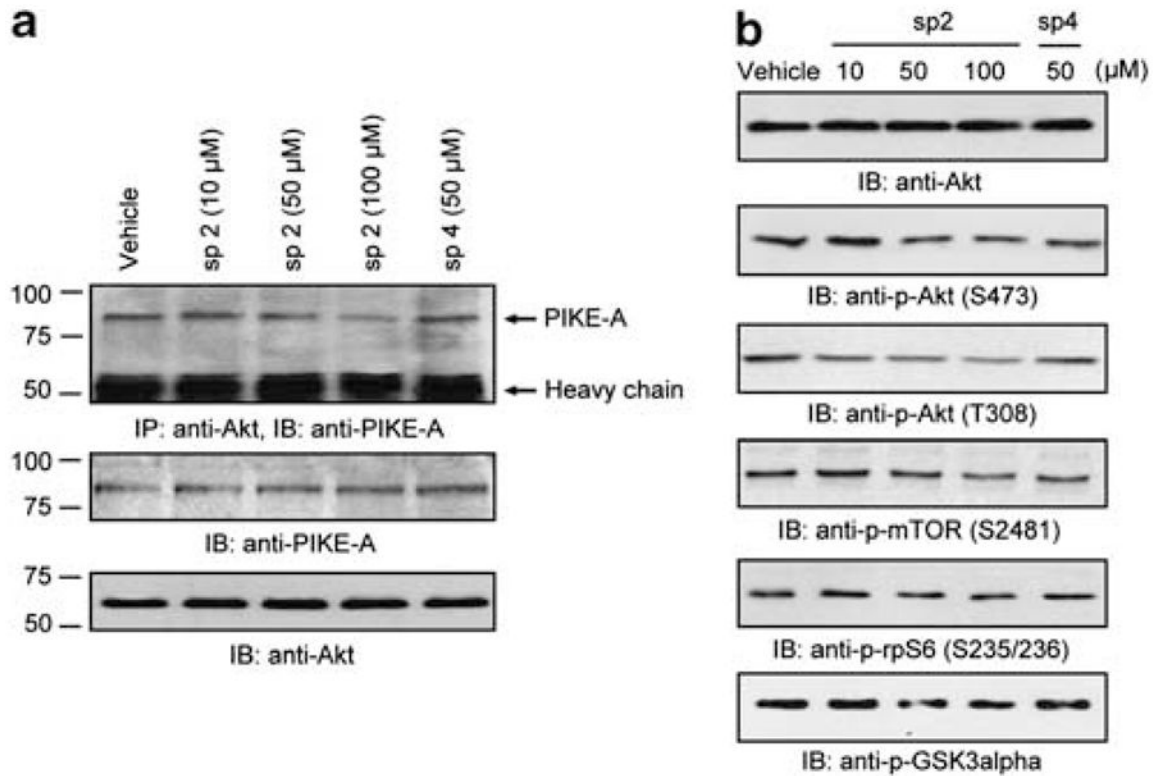


**Figure 7.**

sp2 inhibits the endogenous interaction between PIKE-A and Akt and signaling downstream of Akt. **(a)** co-immunoprecipitate assay was used to validate the effect of sp2 on the interaction of PIKE-A and Akt. LN-Z308 cells were treated with the indicated concentration of sp2 for 16 h. The cell lysate was collected and 1 mg of cell lysate was incubated with 1  $\mu$ g of rabbit polyclonal anti-Akt antibody. Thirty micrograms of whole cell lysate was used as input. The coprecipitated proteins were analyzed with an anti-PIKE-A antibody. The expression of PIKE-A and Akt were verified by immunoblot analysis. Sp2 inhibited the interaction of PIKE-A and Akt in a dose-dependent manner. **(b)** sp2 affected Akt activity via the disruption of PIKE-A/Akt. Activation of signaling downstream of Akt was detected using immunoblotting analysis. Sp2 inhibited Akt activity and the phosphorylation of Akt substrates, which is consistent with the disruption of the interaction between PIKE-A and Akt.